Sports Eng (2009) 11:165–175
DOI 10.1007/s12283-009-0020-9

ORIGINAL ARTICLE

A three-dimensional forward dynamics model of the golf swing

Sasho James MacKenzie · Eric J. Sprigings

Published online: 2 July 2009

Abstract Previously, forward dynamic models of the golf swing have been planar, two-dimensional (2D) representations. Research on live golfers has consistently demonstrated that the downswing is not planar. This paper introduces and evaluates the validity of a 3D six-segment forward dynamics model of a golfer. The model incorporates a flexible club shaft and a variable swing plane. A genetic algorithm was developed to optimise the coordination of the model's mathematically represented muscles (torque generators) in order to maximise clubhead speed at impact. The kinematic and kinetic results confirmed previous findings on the proximal to distal sequencing of joints and the muscles powering those joints. The validity of the mathematical model was supported through comparisons of the model's swing kinematics and kinetics with those of a live golfer.

1 Introduction

Over the past 40 years, the golf swing has been analysed using kinematic [1], inverse dynamic [2] and forward dynamic [3] methods. The appropriateness of the method depends on the research question being addressed. For example, a kinematic analysis provides a description of the motion and is suitable for describing the orientation of a golfer's swing plane [1]. An inverse dynamic method estimates the underlying kinetics for a particular swing and, as one example, is appropriate for estimating the torque acting at the wrist during the downswing [4]. Forward dynamic methods widen the scope of possible research questions by permitting "what if" questions to be investigated [5]. Provided the forward dynamic model is valid, a researcher can investigate such things as the influence, on clubhead speed, of an optimally delayed wrist torque [6]. Regardless of the method, most researchers have made simplifying assumptions to make the analysis tenable. The key is to ensure that the simplification is inconsequential to the particular question being addressed.

A recurrent simplification in the golf swing literature has been the assumption that the downswing can be represented as a movement occurring in a single constant plane [3, 6–16]. However, there is research which suggests the downswing is not planar. Vaughan [4] and Neal and Wilson [2] performed three-dimensional (3D) inverse dynamic analyses of the golf swing which described the kinetics at the golfer's wrist; however, perhaps more relevant to future golf swing modelling research, both studies concluded that the shaft did not move in a constant plane. Vaughan [4] stated that the plane was nearly constant during the last half of the downswing but variable during the first. Conversely, Neal and Wilson [2] suggested the opposite and that the club moved in one plane only for the first half of the downswing. Performing a kinematic analysis, Coleman and Rankin [1] conducted a study which measured the 'left-arm plane' of the golfer's motions and the position of the club relative to that plane. They concluded that the golfer's motions in the downswing were not planar, and the motions of the club were not coincident with the plane established by the motion of the golfer's lead arm and trunk. Measuring an impressive number of 84 golfers, Nesbit [17] reported that the downswing does not take place in a fixed plane. Based on these findings, it

S. J. MacKenzie (✉)
Department of Human Kinetics, St. Francis Xavier University,
PO Box 5000, Antigonish, NS B2G 2W5, Canada
e-mail: smackenz@stfx.ca

E. J. Sprigings
College of Kinesiology, University of Saskatchewan,
Saskatoon, Canada

appears that the club and lead arm are not coplanar and that the plane they move in throughout the downswing is not constant.

While being forward dynamic in nature, Nesbit's model [17] differed from early forward models [3, 9, 14] in that the model was driven by the kinematic patterns of a real golfer. Nesbit captured the 3D kinematics of a swing, fitted each joint angular displacement series with a cubic spline and used these splines to drive the movement of the model. The study provided a thorough kinematic and kinetic description of the swings of 84 separate golfers. While the forward model served as verification to Nesbit's data collection and analysis procedure, it appears his results could have been generated with an inverse dynamics model alone. Recently, Kenny et al. [18] conducted a study, with a methodology similar to that of Nesbit, to investigate the transfer of kinetic energy through the golfer. Kenny et al.'s methodology included an extra step which involved using the captured 3D kinematic data to "train" muscle joint torques in a golfer model. The joint torques were then employed to drive the forward dynamic model. A major finding from their analysis, of a single category 1 golfer, was that the kinetic energy of the arms peaked first suggesting that the optimal coordination of sequencing was not proximal to distal. Of note is their use of the term optimal. There was no manipulation of the model input variables (computed joint torques) to improve some aspect of the model's output behaviour (clubhead speed). Rather, it must be inferred that, they assumed that their test golfer had an optimal swing. While this is possible, there is no way to confirm it. Ideally, they would have manipulated the activation patterns of the model's "trained" muscles, using actual optimisation techniques, to maximise clubhead speed. Following this optimisation, an investigation into the kinetic energy sequencing could have been conducted. Showing that their model closely matched the swing of a live golfer demonstrates the validity of the model, but it does not mean that the model has optimal swing kinematics. If the input kinetics driving a forward model were determined from a specific kinematic pattern, then would the forward model not be expected to reproduce the same kinematics? Similar to the findings of Nesbit [17], Kenny et al.'s question of energy sequencing could have been answered using the initially captured kinematic data without employing the forward-driven simulation. It is not clear if their model can be optimised by manipulating the input kinetics in the manner described by earlier researchers employing forward dynamics and optimisation [19–21]. Although not employed for this purpose, perhaps the major value of Kenny et al.'s model lies in its ability to demonstrate the precise patterns of activation of individual muscles.

While inverse dynamic studies, and the limited forward dynamic studies just described, have advanced the understanding of the golf swing, they are primarily descriptive in nature and as such are restricted in their capacity to test theories. For example, they are not well suited to answer questions such as, "How would clubhead speed change if the golfer exerted no wrist torque during the downswing?" However, with the appropriate model, it is possible to alter the representative muscle activity patterns and answer questions such as the one posed above. Further, it is possible to incorporate an optimisation scheme that conducts a search for the particular muscle activity pattern that yields the 'best' kinematics. While not prone to experimental error, forward dynamic models are susceptible to structural validity concerns. That is, how well does the model physically represent the actual system?

It seems unlikely that a 2D model could provide a valid means for investigating the behaviour of the golf club shaft. This premise is based on the fact that, during the downswing, the club rotates approximately 90° about the longitudinal axis of the lead arm. Despite this fact, the role of shaft stiffness in the golf swing has previously been investigated using 2D forward dynamic models [11, 15, 22]. Perhaps the most-cited study on the role of shaft stiffness is that of Milne and Davis [11], which employed a similar 2D model as that of Budney and Bellow [23], but also incorporated a mathematical representation of shaft bending so as to evaluate the role of shaft stiffness. Milne and Davis concluded that shaft flexibility does not play an important dynamic role in the golf swing. However, there is an important validity concern with the mathematical model developed by Milne and Davis that stems from their attempt to model the 3D nature of shaft dynamics. Milne and Davis realised that an essential requirement of a simulation of shaft bending was that it be 3D. They stated that the main reason for this is that the centre of mass of the clubhead does not lie on the projected line of the shaft. Although presented in a vague fashion, it appears that clubhead rotation about the longitudinal axis of the lead arm was incorporated into their simulation in the following way. From live golfer tests, the distance of the centre of mass of the clubhead from the projected shaft line in the swing plane was determined as a function of the angular position of the shaft. The centre of mass of the clubhead was constrained in their 2D simulations to change its position relative to the shaft as a function of wrist angle. Basically, Milne and Davis developed a 2D forward dynamics model in an attempt to resolve a 3D dynamics problem. The applied torques in the system acted in a single plane, and the inertial properties of the system's segments were only expressed for motion in a single plane. According to classical dynamics, the change in motion of a body does not occur without the application of a force or torque. In reality, some mechanism, perhaps a muscular

torque, must cause the clubhead to rotate about the longitudinal axis of the lead arm in the plane of the swing. Such a mechanism would also have an effect on shaft bending. This mechanism was not represented in the model employed by Milne and Davis and therefore its effect on shaft bending cannot be evaluated.

Based on our review of literature, the golf swing is fundamentally 3D, not planar. Further, any model that attempts to investigate the underlying kinetics of the swing, and the resulting club shaft dynamics, should represent the 3D motion of the golfer and club.

The main purpose of this paper was to develop a 3D forward dynamics model of the golf swing to satisfy this condition. The model's validity was tested by comparing its kinematic and kinetic output to the swing of a live golfer. Following validation, the model was optimised to maximise clubhead speed at impact. The general kinematic and kinetic profiles are reported and compared to findings in the literature.

2 Methods

2.1 Live golfer data collection

A category 1 male golfer (1.83 m, 80 kg and 3 handicap) was used to test the validity of the model. Prior to participating, the participant signed a document of informed consent. The research was approved by the University of Saskatchewan Research Ethics Board. The participant completed a warm-up consisting of ten swings with a driver in which a golf ball was hit into a net from a tee in a laboratory setting. The driver used had a total mass of 310 g and was fitted with a 'regular' shaft. According to the USGA Rules of Golf measurement convention, the driver was 116.5 cm in length [24]. The participant was instructed to swing consistently from shot to shot and to swing as they normally would on the golf course. Following the warm-up, the participant completed six 'well-executed' drives which were captured using a high-speed digital video camera (MotionScope PCI 1000) at a sampling rate of 500 fps and a shutter speed of 1/1,500 s. If the participant felt a particular drive was not well executed, then that trial was repeated. To orient the axis of the lens in a position that was approximately perpendicular to the swing plane, the camera was placed 5.1 m away horizontally and 5.5 m above ground level. Access to a single high-speed camera limited the kinematic data collection to only two dimensions. A high frame rate is necessary to capture the high-speed movements of the downswing. The use of a multiple camera kinematic data collection system would have been preferred.

The video of each swing was analysed using the motion analysis software HU-M-AN^{TM}. Displacement data throughout the swing were generated by manually digitising points on the golfer's right shoulder (lateral edge of acromion), left shoulder (lateral edge of acromion), left wrist (styloid process of the radius) and clubhead (at the hosel). These four points defined a three-segment model (torso, lead arm and club) which could be analysed in HU-M-AN^{TM}. This collection model was chosen to permit comparison of the live golfer results to that of the forward dynamics model described later. The raw coordinate data were low-pass filtered using HU-M-AN's built-in fourth-order recursive Butterworth filter. Cut-off frequencies, ranging from 5 to 19 Hz, were individually selected for each of the X and Y coordinate data sets for each point based on their residual plots [5]. Following smoothing, the absolute angular displacements of the torso, lead arm and club were calculated. The swing that resulted in the highest clubhead speed at impact was selected to test the validity of the model. The participant demonstrated a repeatable swing with an average clubhead speed of 39.9 $\pm$ 0.5 m/s.

2.2 Model geometry, rotations and constraints

Kane's commercial software package, Autolev^{TM}, was used to generate the 3D equations for a six-segment (torso, arm and four club segments) mathematical model of a golfer (Figs. 1, 2). Such a model can represent the four primary motions executed in the downswing: torso rotation, horizontal abduction at the shoulder, ulnar deviation at the wrist and longitudinal rotation about the lead arm

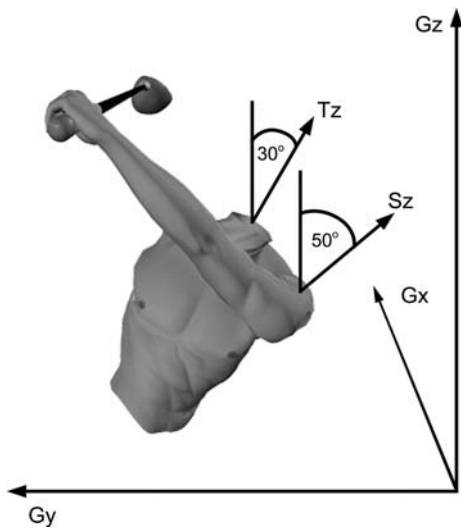

Fig. 1 The initial configuration for the 3D, six-segment model used to simulate the downswing. The global inertial reference frame, G, formed the basis for the model's motion with G_x directed towards the target. The *Torso* was constrained to rotate about axis T_z, while the *Shoulder* was constrained to have rotation about the S_z axis

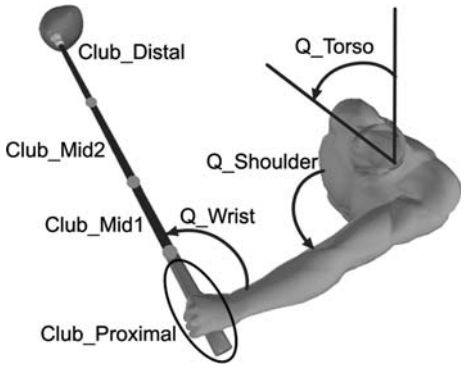

Fig. 2 Depiction of the convention used to express the angular position of the *Torso*, *Shoulder* and *Club_Proximal*, the most proximal club segment. The directions of the arrows indicate positive rotation. The club was modelled as four rigid segments connected by rotational spring-damper elements

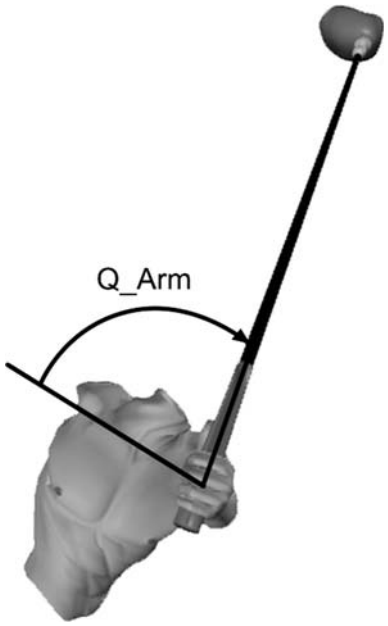

Fig. 3 Convention used to express the arm's longitudinal rotation. *Q_Arm* was initially set to 0° at the top of the backswing. If the model was placed in the typical address position assumed by a professional golfer, then *Q_Arm* would be approximately 90°

[25]. The model parameters, which will be described later, were based on the test golfer and the driver used during the live golfer tests. The following is a description of the 3D model's representation in Autolev^{TM}.

A global inertial frame of reference, *G*, was created as a basis for the model's motion. G_x was horizontal and oriented towards the hypothetical target, G_z was in the positive vertical direction, and G_y was directed according to the right-hand-rule convention (Fig. 1). The *Torso* segment was constrained to rotate about an axis, T_z, angled at 30° from the vertical (Fig. 1). The angular position of the *Torso* was defined by the angle *Q_Torso* (Fig. 2).

The *Arm* segment was modelled as a straight rigid body with the elbow joint fixed at 180°. The *Arm* was able to perform horizontal adduction-abduction as well as internal–external rotation about its own longitudinal axis. The adduction–abduction movement was modelled by affixing an intermediate reference frame, *Shoulder*, to the *Torso* segment. The *Shoulder* reference frame was constrained to rotate about an axis, S_z, angled at 50° from the vertical (Fig. 1). The angular position of the *Shoulder* was defined by the angle *Q_Shoulder* (Fig. 2). The *Arm* segment was affixed to the *Shoulder* reference frame and, therefore, moved in the adduction–abduction plane with the *Shoulder* reference frame. In addition, the *Arm* rotated about its own longitudinal axis, which represented a combination of shoulder internal–external rotation and forearm pronation–supination. This motion was defined by the angle *Q_Arm* (Fig. 3).

The hand and most proximal club segment were combined to represent a single segment, *Club_Proximal* (Fig. 2). Nesbit also combined the mass and inertia properties of the hand with the most proximal club segment [17]. *Club_Proximal*, connected to the *Arm*, was constrained to only have motion about a representative wrist ulnar–radial deviation axis. The wrist ulnar–radial deviation motion was defined by the angle *Q_Wrist* (Fig. 2).

The four segments of the modelled club were connected in series by three rotational spring-damper elements. Due to the length of the closed form solution of the dynamical equations representing the model, the number of shaft segments was limited to four. The inclusion of additional shaft segments resulted in the computer program becoming too large to compile into an executable file. The modelled shaft will be described in more detail in a subsequent publication. The shaft was capable of deflecting about two axes (Fig. 4). Deflection along the *Y* axis represented lead/lag motion, while deflection along the *X* axis represented toe-up/toe-down motion. The magnitude of shaft deflection was calculated by determining the displacement of the clubhead relative to its theoretical position if the shaft were rigid (Fig. 5). Test simulations conducted in the development of the model used in this paper, indicated that the shaft twisted about its longitudinal axis less than 0.2°, yet incorporating this extra degree of freedom approximately tripled the simulation time. The test simulations consisted of executing optimised downswings of the complete model described later. The torsional stiffness of the modelled club was based on industry standard torque measurements taken on the driver used in the live golfer testing described later. Compared to the magnitude of deflection about the other axes, twisting about the longitudinal axis during the downswing is minimal (<0.6°) and was, therefore, not incorporated into the model [26]. It is important to note

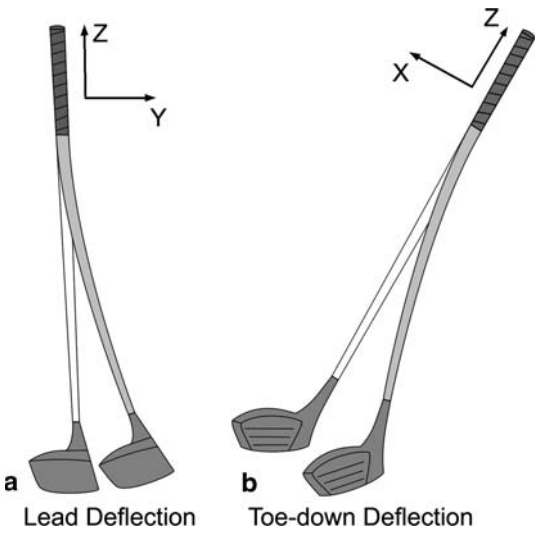

Fig. 4 The modelled shafts were capable of deflecting about two axes. **a** Deflection along the *Y* axis represents lead/lag motion. **b** Deflection along the *X* axis represents toe-up/toe-down motion

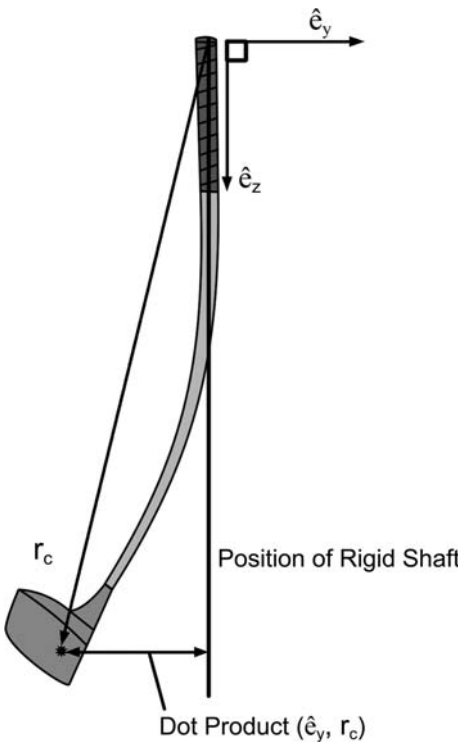

Fig. 5 Method used to calculate lead/lag shaft deflection along the *Y* axis of the shaft. A unit vector ($\hat{\mathbf{e}}_\mathbf{z}$) representing the axial direction of a rigid shaft was constructed along the length of the most proximal club segment, *Club_Proximal*. A unit vector ($\hat{\mathbf{e}}_\mathbf{y}$) perpendicular to the rigid shaft vector ($\hat{\mathbf{e}}_\mathbf{z}$) was formed along the *Y* axis. A third vector ($\mathbf{r_c}$) was defined from the proximal end of the club to a point in the clubhead that represented an extension of the shaft to the depth of clubhead's centre of gravity. A measurement of lead/lag deflection was found by taking the dot product of $\hat{\mathbf{e}}_\mathbf{y}$ and $\mathbf{r_c}$. A similar process was used for calculating toe-up/toe-down deflections

that, without incorporating shaft twisting into the model, the clubface will still be 'open' when the clubhead is deflected in the lag direction, and 'closed' when the clubhead is deflected in the lead direction [25]. The relationship between clubface orientation and shaft deflection (about the *X* and *Y* axes) is mediated by the static lie angle of the club. For example, since the shaft inserts into the clubhead at an angle from the vertical, lead deflection (Fig. 4) will result in both added loft as well as a closed clubface.

2.3 Muscle torque generators

Four torque generators, which adhered to the activation rates and force–velocity properties of human muscle, were incorporated to provide the model with the capability of controlling energy to the system [14]. A single torque generator was incorporated for each rotational degree of freedom in the golfer portion of the model, for a total of four torque generators. The force–length property of muscle was not incorporated into the torque generators as it was expected to play a second order role [27]. Determining the output from each torque generator was a two-step process. The first step incorporated the activation rate of muscle and took the form

$$T = T_\mathrm{m}\left(1 - \mathrm{e}^{-t/\tau_\mathrm{act}}\right) \tag{1}$$

To incorporate the deactivation time of muscle when the torque generator was disengaged, it took the form

$$T = T_\mathrm{m}\left(1 - \mathrm{e}^{-t/\tau_\mathrm{act}}\right) - T_\mathrm{m}\left(1 - \mathrm{e}^{-t'/\tau_\mathrm{act}}\right) \tag{2}$$

where

T_m	maximum isometric torque
τ_act	activation time constant
τ_deact	deactivation time constant
t	total time from start of torque generator activation
t'	total time from disengagement of torque generator

The force–velocity property of muscle can be incorporated by scaling the value of *T* after the activation rates have been factored into the muscle model [28] (Eq. 3). Sprigings and Neal [14] have since incorporated this method into a forward dynamic simulation of the golf swing.

$$T_\mathrm{new} = T\frac{(\omega_\mathrm{max} - \omega)}{(\omega_\mathrm{max} + \Gamma\omega)} \tag{3}$$

where

ω_max	the torque generator's maximum unloaded rate of shortening
ω	the torque generator's current rate of shortening

Table 1 Parameter values for the muscular torque generators used to power the model

Generator	T_m (N m)	τ_{act} (ms)	τ_{deact} (ms)	ω_{max} (rad/s)	Γ
M_Torso	200	20	40	30	3.0
M_Shoulder	160	20	40	30	3.0
M_Arm	60	20	40	60	3.0
M_Wrist	90	20	40	60	3.0

Γ a shape factor for the curvature of the torque/velocity relationship

While the muscle torque generators do not represent specific muscles, they do represent the collective actions of groups of muscle acting at each joint. The parameter values for each torque generator were estimated based on the groups of muscles they would likely represent (Table 1).

2.4 Model parameters

Parameter values for the golfer model were based on the golfer used in the live tests (Table 2). Segment masses and moments of inertia were calculated using the regression equations provided by Zatsiorsky in Appendix A2.8 of his book [29]. The regression equations required specific lengths and diameters to be measured on the live golfer. Parameter values for the club segments were based on taking direct measurements of the driver used in the live golfer tests (Table 2). Further details on model parameters have been previously presented [25, 30].

2.5 Model validation

The model's validity was tested by instructing the model to generate a swing similar to the live golfer and measuring the fit between the simulated and real swing kinematics. This was accomplished in the following manner. The angular displacement curves (torso, lead arm and club) captured from the live golfer were each fitted with a sixth degree polynomial as a function of the downswing time. Each polynomial had an $R^2 > 0.99$ relative to the raw data demonstrating a very close fit. For the purpose of this validation test, the start of the downswing was defined by the first sign of torso counter-clockwise rotation. The model was given the same initial starting configuration as the live golfer at $t = 0$ s. An optimisation scheme was employed which minimised the root mean square error (RMSE) between the absolute angular displacement of the model's segments and that of the live golfer as represented by the polynomial functions. The optimisation scheme functioned by manipulating ten control variables, consisting of the onset and duration times for the four torque generators as well as two scaling variables for T_m and ω_{max}. The optimisation search engine was developed by the lead author and employed an evolutionary algorithm approach, as generally expressed in theory by Michalewicz [31]. Further details regarding the optimisation methods have been previously published [30].

2.6 Model optimisation

The previous section described how the model's muscular coordination strategy was optimised to match the resulting kinematics with those of a live golfer. However, it is possible that the live golfer's swing was not optimal; therefore, a second optimisation was conducted. The model's goal, in this second optimisation, was to maximise horizontal clubhead speed at impact with the golf ball. The objective function was composed of the horizontal clubhead speed at impact minus any penalty variables accumulated during the simulated golf swing. Penalties were incurred if the model performed movements that were not executable by a human golfer, such as having the arm segment pass through the torso segment. Penalties were also incurred if the model was not in a proper position at impact, such as having the clubface misaligned with the target. Eight control variables, consisting of the onset and duration times for the four torque generators, were optimised to determine maximum horizontal clubhead speed at impact using an algorithm similar to that described in the

Table 2 Golfer model segment parameters

Segment	Mass (kg)	Length (cm)	CM_x (cm)	CM_y (cm)	CM_z (cm)	I_x (kg cm^2)	I_y (kg cm^2)	I_z (kg cm^2)
Torso	34.61	40.0	–	20.0	–	–	–	3655
Arm	3.431	60.0	–	–	26.1	1076	1096	58.06
Club_Proximal	0.534	30.0	–	–	5.6	11.81	11.81	6.287
Club_Mid1	0.021	30.0	–	–	14.9	1.579	1.579	0.009
Club_Mid2	0.020	30.0	–	–	14.9	1.509	1.509	0.005
Club_Distal	0.213	22.5	5.2	−4.7	21.7	6.621	8.792	4.200

CM_x, CM_y and CM_z refer to the position of the centre of mass along axes x, y and z of each segment

I_x, I_y and I_z, refer to the moments of inertia of each segment about axes x, y and z of the segment

previous section. The initial configuration of the golfer-club model was as depicted in Fig. 1. The starting values for *Q_Torso*, *Q_Shoulder*, *Q_Arm* and *Q_Wrist* were 0°, 20°, 0° and 70°, respectively. Figures 2 and 3 reveal the measurement conventions for these angles. An initial angular velocity of 5 rad/s, in the backswing direction, about the T_z axis was also given to all segments of the model, so as to simulate the dynamic transition from the backswing into the downswing.

3 Results and discussion

3.1 Model validation

Access to a single high-speed camera limited the model's validation to two dimensions. This meant that the longitudinal rotation of the model's lead arm could not be quantitatively compared to that of the live golfer.

The model was able to closely match the kinematics of the live golfer (Fig. 6). The RMSE values for the torso (1.25°), arm (0.66°) and club (1.53°) absolute angular displacement curves reveal the high level of agreement. The R^2 values for the associated model and live golfer displacement curves were all greater than 0.99. The radial force acting at the wrist also showed close agreement (RMSE = 14.4 N, $R^2 = 0.98$) and improved as impact approached (Fig. 6). The clubhead speed curves (not shown) for the simulated and live swings were also in close agreement (RMSE = 1.32 m/s and $R^2 > 0.99$). The live golfer generated a clubhead speed at impact that was 0.04 m/s faster than that of the model. In terms of clubhead speed, the fit of this model to live golfer results appears as good as that of Kenny et al. [18], who reported a RMSE of 1.93 m/s and a difference in peak clubhead speed of 1.99 m/s. The fit of the 3D trajectory data reported by Kenny et al. appears to be in spherical coordinates making it difficult to compare with our results. It is important to note that, in this study, the live golfer kinematics was not used in an inverse dynamic sense to determine the kinetics of the model. The results of the validation test indicate that the model is suitable to undergo further optimisation from which inferences can be made regarding an optimal downswing.

3.2 Model optimisation

The following results describe the kinematics and kinetics of the golfer model following optimisation for maximum clubhead speed at impact. The angular displacement histories produced by the simulation model demonstrated a proximal to distal sequencing of movement (Fig. 7), which is consistent with the 2D kinematic results reported by

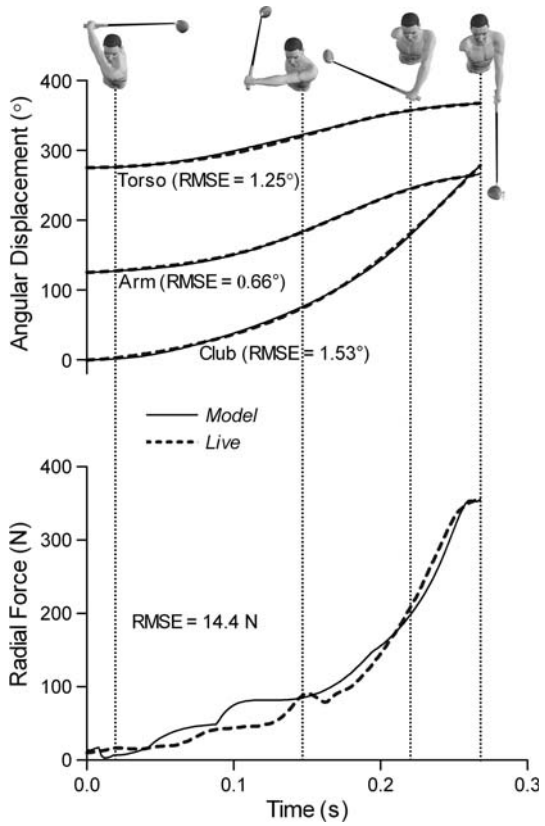

Fig. 6 *Top* absolute angular displacement of the model's segments in comparison to that of the live test golfer. Angles are measured from the right horizontal. Root mean square error is also provided as an indication of the model's fit to the live golfer kinematics. *Bottom* comparison of the radial force acting at the wrist throughout the downswing swing for the model and live test golfer. The RMSE provides an indication of the model's fit to the live golfer kinetics

previous researchers [14, 32, 33]. From approximately 0.1–0.2 s, the *Q_Arm* curve dips in the negative direction. In the popular golfing literature, this would be referred to as 'dropping the club below the swing plane'. This negative rotation about the longitudinal axis of the lead arm is the result of gravity acting on the mass of the club and producing a torque about the lead arm. A review of Fig. 1 will help to clarify this point. Following this dip, the *Arm* quickly externally rotates about its longitudinal axis to square the clubface for impact.

Clubhead velocity in the G_x direction was 41.9 m/s (94.3 mph) at impact (Fig. 7). This clubhead speed, while approximately 7 m/s slower than PGA professionals, is within the range previously reported in the literature and very close to that of Milne and Davis (41.4 m/s) [11]. It is expected that increasing the simulated clubhead speed by increasing the input torque values, would increase the magnitudes of some variables reported later, but not the conclusions reached. It is interesting to note that the model employed an inside-to-outside clubhead path, which is characteristic of expert golfers. This is clear from the G_y

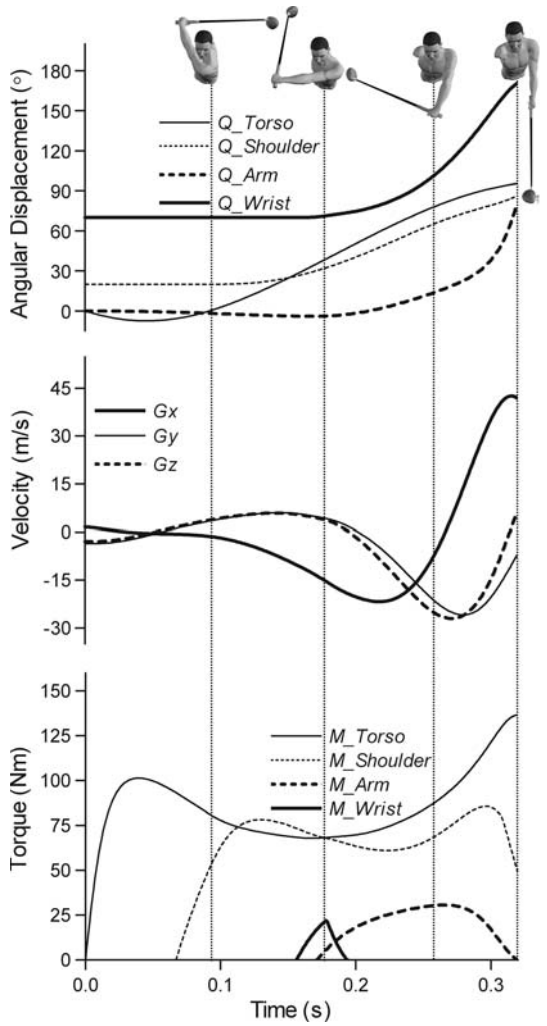

Fig. 7 *Top* segment angular displacements for the optimised golfer model. *Middle* plot of clubhead velocity components directed along each axis of the global inertial reference frame. G_x was directed toward the target, G_y was directed perpendicular to the target line running behind the golfer, and G_z was in the positive vertical direction. *Bottom* torque output from the muscular torque generators for the optimised golfer model

component of clubhead speed (−7.2 m/s) at impact. The clubhead was also travelling with a velocity component (6.1 m/s) in the vertical direction, which is typical of a swing made while using a driver off the tee deck.

The output from each of the muscular torque generators was consistent with the force–velocity properties of muscle in that the torque output diminished as the relative joint angle speed increased. The optimal activation of the torque generators was in a proximal to distal pattern with *M_Torso* being activated at $t = 0$ s and remaining active for the entire downswing (Fig. 7). *M_Torso* peaked at 136 N m which is well under the maximum torso rotation torque of 192 N m reported in the literature [34]. *M_Shoulder*, which produced an arm abduction torque, was activated at approximately 0.07 s and remained active for the duration of the downswing. *M_Shoulder* peaked at 85 N m which is slightly greater than maximum shoulder abduction torques (∼80 N m) previously reported [35]. However, this was as expected since T_m for *M_Shoulder* was doubled to compensate for the lack of a trailing arm. *M_Wrist* (i.e. ulnar deviation) was initiated at approximately 0.16 s and was active for a relatively short duration. Ulnar deviation torque is expected to play a minor role in increasing clubhead speed since, near impact; it produces clubhead motion which is perpendicular to the intended direction of ball flight. *M_Arm*, the external rotator of the *arm*, was the final muscle torque generator to be activated (0.17 s) and it remained engaged for the duration of the downswing. It should be noted that the model neglects any energy influence from the legs. This has probably resulted in slightly greater outputs from the aforementioned muscular torque generators.

Coleman and Rankin [1] showed that, for a 5 iron swung by a professional golfer (Participant 1 in their study), the left-arm swing plane showed a slight increase in angle before peaking at approximately 138° and then steadily decreasing to an angle of approximately 103° at impact. The swing plane angle was measured from the right horizontal (negative G_y in Fig. 1). Thus the swing plane for their Participant 1 increased in steepness by approximately 35° throughout the downswing. The swing plane angle for the model in our study, using a driver, also increased in steepness by approximately 35° as it decreased from a maximum angle of 165° to an angle of 130° at impact (Fig. 8). The swing plane angle followed the same general pattern as presented by Coleman and Rankin (for Participant 1 who had a 0 handicap), but was consistently 'flatter' at all points during the swing because of the added length

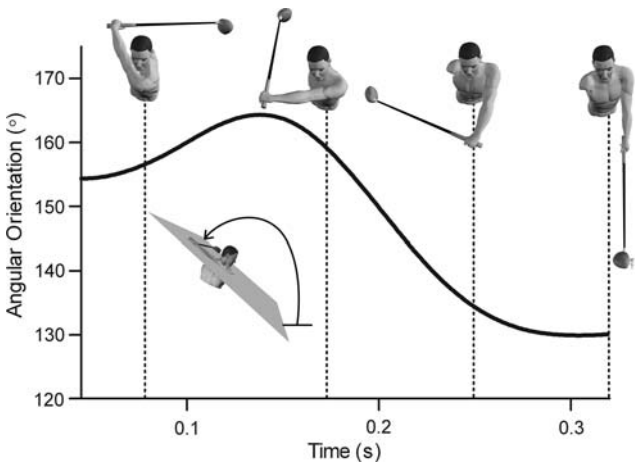

Fig. 8 Time history graph of the left-arm swing plane as measured from the negative G_y axis (right horizontal) during the optimised downswing simulation. This measurement system was the same as that used by Coleman and Rankin [1]

of the driver over a 5 iron. The driver swing plane angle at impact for this study (130.1°) was also in the range reported by Williams and Sih [36] through the impact area (131.5 ± 3.9°); Williams and Sih did not report swing plane for the entire downswing.

As shown by the results of Butler and Winfield [26], it is difficult to compare the exact magnitudes of shaft deflection during the downswing between golfers, or between an optimised model and a golfer. Butler and Winfield reported differences in the magnitude of shaft deflections during the swing of three golfers using the same club and who all generated the same clubhead speed at impact (Appendix). However, there were certain characteristics of each swing that held true. The highest magnitude of shaft deflection occurred in the toe-up direction at the start of the downswing. Maximum toe-up deflection occurred before maximum lag deflection. Also, the shaft was always deflected in the toe-down and lead directions at impact. These characteristics of shaft deflection during the downswing are evident in Fig. 9 of the current paper. Lee et al. [37] developed an advanced shaft strain measurement system mounted in the actual club. Their patterns of strain, reported in both the lead/lag and toe-up/toe-down directions, showed excellent correspondence with the shaft deflection results in our study. Unfortunately, they only reported strain measurements and did not provide corresponding clubhead displacement measurements. However, the following quotes from Lee et al. could easily be used to describe the curves in Fig. 9 of the current paper: "the lead/lag strain reaches its maximum value after the maximum toe-up strain." With regards to lead/lag deflection, "the shaft goes from a bent backwards position to a bent forward position at impact". Also, "the toe-down strain becomes negative just prior to impact."

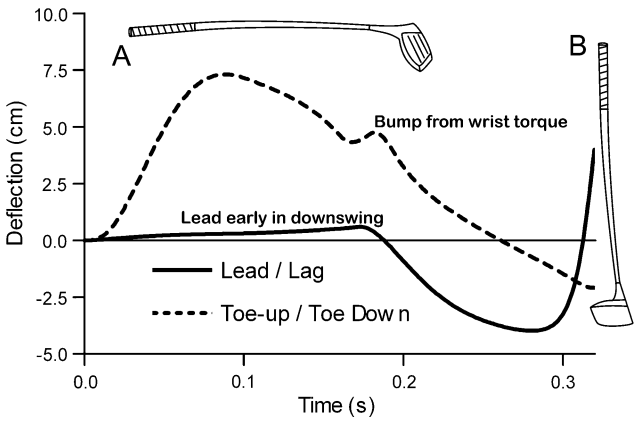

Fig. 9 Time history graph of toe-up/toe-down and lead/lag deflections during the optimised downswing simulation. Club '*A*' accurately depicts a driver with 8 cm of toe-up deflection. Club '*B*' accurately depicts a driver with 5 cm of lead deflection

A comparison of the simulated shaft deflections at key points in the downswing can be made to the swing of Golfer 3 from Butler and Winfield (Appendix). For example, Butler and Winfield reported peak deflections in the toe-up direction of 9.1 cm. In this study, the greatest shaft deflection (7.3 cm) occurred in the toe-up direction during the initial stage of the downswing (Fig. 9). This deflection was primarily a result of the torques generated by *M_Torso* and *M_Shoulder*. The shaft recovered from the toe-up deflection and moved steadily into a maximum toe-down deflected position (−2.1 cm) at impact (Fig. 9). Butler and Winfield reported a larger maximum toe-down deflection at impact (−4.3 cm). The move into a toe-down deflected position was the result of centripetal (radial) force acting on the offset position of the clubhead's centre of mass as well as recoil from the initial toe-up deflection. At approximately 0.18 s, the effect of *M_Arm* engaging to square the clubface for impact becomes evident. This torque resulted in a maximum lag deflection (−4.0 cm) just 0.04 s prior to impact. Over the final 0.04 s, the club quickly moved from its maximum lagging position into its maximum leading position (4.0 cm) at impact (Fig. 9). This action supports the possibility of the golf shaft acting as a spring to increase the relative velocity of the clubhead. Butler and Winfield measured a similar maximum lead deflection at impact of approximately 3.8 cm.

The model's shaft deflections closely resembled those of Golfer 3 from Butler and Winfield [26]; however, we believe that key features in the model's shaft deflections are also evident in the swings of Golfer 1 and Golfer 2 (Appendix). For example, for the first half of the downswing the influence of radial force resulted in a small lead deflection in the model (Fig. 9) and a similar deflection at the same point in the downswing can be seen during the swing of Golfer 1 (Appendix). The engagement of *M_Wrist* is evident from the small positive bump in toe-up deflection at approximately 0.18 s in the model, while a similar bump can be seen during the swing of Golfer 2 (Appendix). Also, all three swings illustrated by Butler and Winfield showed that maximum lag deflection occurred approximately 0.05 s before impact which agrees well with the results from our simulation (∼0.04 s).

Teu et al. [38] stated the importance of external rotation of the arm and point out that these motions are not accounted for in a 2D approach. The use of a 3D model has two clear implications to the clubhead deflection results (Fig. 9). First, it demonstrates that if a golfer applies a torque about the longitudinal axis of the lead arm, a meaningful magnitude of deflection occurs in the lag direction. While this lag deflection is not initially "in the plane of the swing" it will have influence along the intended target line by the time the clubhead squares up for impact with the ball. Second, it demonstrates that the initial

deflection in the toe-up direction is inconsequential to clubhead speed. This is so because, at impact, any residual effect from earlier toe-up/toe-down deflections will only be evident in a direction perpendicular to that of the target line.

4 Conclusions

A 3D forward dynamics model of the downswing was validated by demonstrating a close fit to the swing kinematics ($R^2 > 0.99$) and kinetics ($R^2 > 0.98$) of a low handicap golfer. The activation timing of the model's muscular torque generators was then optimised so as to maximise clubhead speed at impact. The resulting optimal swing agreed well with previous findings. Specifically, segmental sequencing was proximal to distal, the clubhead followed an inside-out path hitting the ball on the upswing, the swing plane increased in steepness as impact approached, and the patterns of shaft deflection were consistent with the most diligent experimental studies in the area. The findings indicate that this 3D model represents the downswing with sufficient accuracy to examine questions that were not possible with previously employed 2D models and methods. For example, how do the "swing plane" and the position of the shaft relative to that plane affect the dynamics of the downswing? A subsequent publication utilises the model to investigate the role of shaft dynamics in the golf swing.

Acknowledgments The authors acknowledge the Natural Sciences and Engineering Research Council of Canada for providing funding support. The authors thank Pierre Gervais for the use of the Biomechanics Lab at the University of Alberta, and his Ph.D. student, Steve Leblanc for helping verify the results via high-speed videoing of a live golfer.

Conflict of interest statement The authors declare that they have no conflict of interest.

Appendix

The following graphs, from Butler and Winfield [26], represent the deflection of the clubhead during the downswings of three different golfers (Fig. 10). Each of the golfers attained the same clubhead speed of 46 m/s at impact. Butler and Winfield used strain gauges which collected shaft deflection data at 50,000 Hz. They used the same conventions as the current paper for describing the direction of deflection. Traces representing shaft twisting, which they found to be minimal (<0.6°) as well as data following impact has not been included on the graphs below; this improved the clarity of the graphs and made them easier to compare to Fig. 9 in the current paper. While each of the swings below has unique deflection characteristics, they also all show the same general pattern as the model used in the current paper.

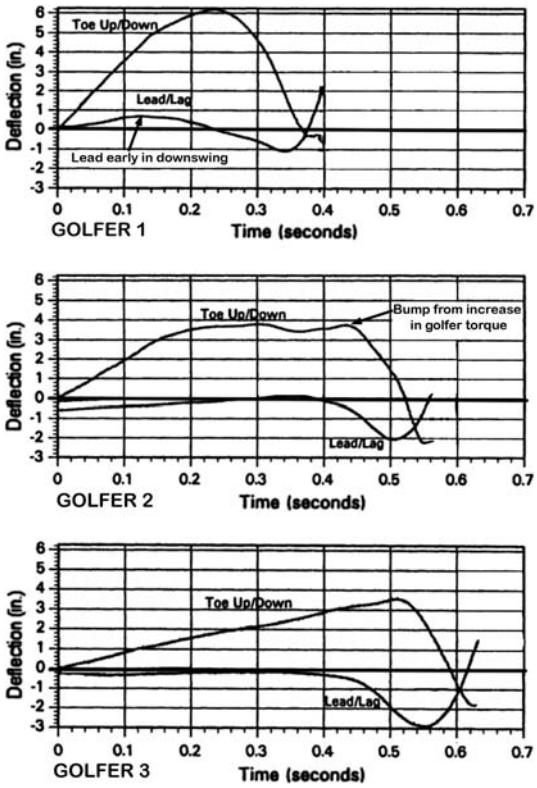

Fig. 10 Toe-up/toe-down and lead/lag deflections during the downswings of three different golfers. All traces end at impact with the ball. Reprinted, by permission, from Butler and Winfield [26, pp 261–262], Figs. 1, 2 and 3

References

1. Coleman SG, Rankin AJ (2005) A three-dimensional examination of the planar nature of the golf swing. J Sports Sci 23:227–234
2. Neal RJ, Wilson BD (1985) 3D kinematics and kinetics of the golf swing. Int J Sports Biomech 1:221–232
3. Lampsa M (1975) Maximal distance of the golf drive: an optimal control study. J Dyn Syst Meas Control 97:362–367
4. Vaughan CL (1981) A three-dimensional analysis of the forces and torques applied by a golfer during the downswing. In: Morecki A, Fidelus K, Kedzior K, Wit A (eds) International series of biomechanics VII-B, 1st edn. University Park Press, Warsaw, pp 325–331
5. Winter DA (2005) Biomechanics and motor control of human movement. Wiley, Mississauga
6. Sprigings EJ, MacKenzie SJ (2002) Examining the delayed release in the golf swing using computer simulation. Sports Eng 5:23–32
7. Chen CC, Inoue Y, Shibara K (2007) Numerical study on the wrist action during the golf downswing. Sports Eng 10:23–31
8. Cochran AJ, Stobbs J (1968) The search for the perfect swing. Morrison & Gibb Ltd, London

9. Jorgensen TP (1970) On the dynamics of the swing of a golf club. Am J Phys 38:644–651
10. Jorgensen TP (1994) The physics of golf. American Institute of Physics Press, New York
11. Milne RD, Davis JP (1992) The role of the shaft in the golf swing. J Biomech 25:975–983
12. Pickering WM, Vickers GT (1999) On the double pendulum model of the golf swing. Sports Eng 2:161–172
13. Sharp RS (2008) On the mechanics of the golf swing. Proc R Soc A 466:1–21
14. Sprigings EJ, Neal RJ (2000) An insight into the importance of wrist torque in driving the golfball: a simulation study. J Appl Biomech 16:356–366
15. Suzuki S, Haake SJ, Heller BW (2006) Multiple modulation torque planning for a new golf-swing robot with a skilful wrist turn. Sports Eng 9:201–208
16. Williams D (1967) The dynamics of the golf swing. Q J Mech Appl Math 20:247–264
17. Nesbit SM (2005) A three dimensional kinematic and kinetic study of the golf swing. J Sports Sci Med 4:499–519
18. Kenny IC, McCIoy AJ, Wallace ES, Otto SR (2008) Segmental sequencing of kinetic energy in a computer-simulated golf swing. Sports Eng 11:37–45
19. Ashby BM, Delp SL (2006) Optimal control simulations reveal mechanisms by which arm movement improves standing long jump performance. J Biomech 39:1726–1734
20. Pandy MG, Zajac FE, Sim E, Levine WS (1990) An optimal control model for maximum-height human jumping. J Biomech 23:1185–1198
21. Pandy MG, Zajac FE (1991) Optimal muscular coordination strategies for jumping. J Biomech 24:1–10
22. Miao T, Watari M, Kawaguchi M, Ikeda M (1998) A study of clubhead speed as a function of grip speed for a variety of shaft flexibility. In: Cochran AJ, Farrally MR (eds) Science and Golf III: proceedings of the World Scientific Congress of Golf, 1st edn. Human Kinetics, Leeds, pp 554–561
23. Budney DR, Bellow DG (1979) Kinetic analysis of a golf swing. Res Q 50:171–179
24. United States Golf Association (2007) The rules of golf. USGA, USA
25. MacKenzie SJ (2008) Three dimensional dynamics of the golf swing: a forward dynamics approach with a focus on optimizing shaft stiffness. VDM Verlag, Saarbruecken
26. Butler JH, Winfield DC (1994) The dynamic performance of the golf shaft during the downswing. In: Cochran AJ, Farrally MR (eds) Science and Golf II: proceedings of the World Scientific Congress of Golf, 1st edn. E & F Spon, London, pp 259–264
27. Caldwell G (1995) Tendon elasticity and relative length: effects on Hill two-component muscle model. J Appl Biomech 11:1–24
28. Alexander RM (1990) Optimum takeoff techniques for high and long jumps. Philos Trans R Soc Lond B Biol Sci 329:3–10
29. Zatsiorsky VM (2002) Kinetics of human motion. Human Kinetics, Windsor
30. MacKenzie SJ (2005) Understanding the role of shaft stiffness in the golf swing. PhD dissertation/thesis. University of Saskatchewan. Saskatchewan, Canada. http://library2.usask.ca/theses/available/etd-12212005-163850/
31. Michalewicz Z (1996) Genetic algorithms + data structures = evolution programs. Springer, New York
32. McTeigue M, Lamb SR, Mottram R, Pirozzolo F (1994) Spine and hip motion analysis during the golf swing. In: Cochran AJ, Farrally MR (eds) Science and Golf II: proceedings of the World Scientific Congress of Golf, 1st edn. E & FN Spon, London, pp 50–58
33. Milburn PD (1982) Summation of segmental velocities in the golf swing. Med Sci Sports Exerc 14:60–64
34. Schultz A, Haderspeck K, Warwick D, Portillo D (1983) Use of lumbar trunk muscles in isometric performance of mechanically complex standing tasks. J Orthop Res 1:77–91
35. Kuhlman JR, Iannotti JP, Kelly MJ, Riegler FX, Gevaert ML, Ergin TM (1992) Isokinetic and isometric measurement of strength of external rotation and abduction of the shoulder. J Bone Joint Surg Am 74:1320–1333
36. Williams KR, Sih BL (2002) Changes in golf clubface orientation following impact with the ball. Sports Eng 5:65–80
37. Lee N, Erickson M, Cherveny P (2002) Measurement of the behavior of the golf club during the golf swing. In: Thain E (ed) Science and Golf IV: proceedings of the World Scientific Congress of Golf, 1st edn. Routledge, London, pp 375–386
38. Teu KK, Kim W, Fuss FK, Tan J (2006) The analysis of golf swing as a kinematic chain using dual Euler angle algorithm. J Biomech 39:1227–1238